Coordinated Expression of MicroRNA-155 and Predicted Target Genes in Diffuse Large B-cell Lymphoma

Deepak Rai, **Shailaja Karanti**, **Inkyung Jung**[*], **Patricia L.M. Dahia**, and **Ricardo C.T. Aguiar**

Division of Hematology and Medical Oncology - Department of Medicine, San Antonio Cancer Institute, University of Texas Health Science Center at San Antonio

[*] *Department of Epidemiology and Biostatistics, San Antonio Cancer Institute, University of Texas Health Science Center at San Antonio*

Abstract

MicroRNAs (miRNAs) attenuate gene expression by pairing to the 3′UTR of target transcripts inducing RNA cleavage or translational inhibition. Overexpression of microRNA-155 (miR-155), measured either at the primary (*BIC* gene) or mature transcript level, was recently described in diffuse large B-cell lymphomas (DLBCL). However, these studies have been limited in size and have not attempt to link miR-155 expression to that of putative target genes. To start to address these issues we examined a collection of 22 well-characterized DLBCL cell lines. The expression of miR-155 is heterogeneous in these cell lines and associates with NF-κB activity. Importantly, we found that the expression of the primary miR-155 transcript reliably reflects that of the functional mature miR-155. Since many gene array platforms include probe sets for the primary miR-155 sequences, these findings allowed us to confidently examine large array-based expression datasets of primary DLBCLs in the context of miR-155 levels. Our investigation revealed that that miR-155 expression segregates with specific molecular subgroups of DLBCL and it is highest in the Activated B-cell (ABC)-type lymphomas. These findings were particularly relevant because these tumors are characterized by constitutive activation of NF-κB signals supporting the data derived from our cell lines. More importantly, using supervised learning algorithms, we identified a robust gene signature driven by the differential expression of miR-155. These profiles contained several gene markers, including predicted targets, consistently downregulated in tumors expressing the high levels of miR-155. Our data start to unveil the genome wide effects of miR-155 expression in DLBCL and indicate the utility of this strategy in the identification and validation of miRNA target genes.

Introduction

MicroRNAs (miRNAs) attenuate gene expression by pairing to the 3′UTR of target transcripts inducing RNA cleavage or translational inhibition [1]. miRNAs are central regulators of various physiologic processes and their disruption is associated with human diseases, particularly cancer [2]. In subsets of B-cell lymphomas and Hodgkin's disease (HD), the expression of microRNA-155 (miR-155), the functional product of the non-coding gene *BIC* (primary miR-155) is abnormally high [3–7]. The oncogenic nature of miR-155 activity was

recently reinforced by the development of tumors with features of high grade lymphoma in Eμ-miR-155 transgenic mice [8]. However, the mechanism by which miR-155 contributes to lymphomagenesis remains unclear and a link between its expression and to that of putative target genes in primary tumors has not been fully established.

MiRNAs are transcribed by RNA polymerase II as transcription units called primary miRNAs (pri-miRNAs) [1]. Pri-miRNAs are cleaved by the Drosha/DGCR8 complex to release a ~ 60–70nt intermediate, the precursor miRNAs (pre-miRNAs). Pre-miRNAs are exported into the cytoplasm and processed by another RNase III, Dicer, giving rise to ~ 22-nucleotide mature miRNA. The mature miRNA is loaded into an effector complex termed RISC (RNA-induced silencing complex) where target mRNAs are inhibited. Given the complexity of this multifaceted process, called miRNA biogenesis, and the still incomplete understanding of miRNA regulation, concerns have been raised as to whether the pri-miRNA transcripts can be used as a reliable surrogate measure for the expression of the functional product, the mature miRNA [9]. Indeed, attempts to define the expression of miR-155 in diffuse large B-cell lymphomas (DLBLC) have interchangeably used the pri-miR-155 (*BIC*) or mature miR-155 [4–7]. And at least in one instance, a limited correlation between these two measurements was suggested [6]. It is important to define this issue because: 1. It will give insight into the biogenesis of miR-155 in this tumor model; 2. It may endorse quantification of pri-miR-155 as a surrogate measure of mature miRNA expression and, 3. It could facilitate the understanding of the role of this miRNA in a genome wide context since pri-miR-155 sequences, as well as those of several other known pri-miRNAs, are included in gene array platforms. The ability to perform these comprehensive analyses has the potential to unveil unsuspected connection between miRNAs, oncogenic signaling pathways and regulatory networks and may lead to the identification and/or validation of directly targeted genes.

Herein, we describe a precise correlation between the primary and mature miR-155 messages in a large collection of DLBCL cell lines. These findings allowed us to confidently examine large array-based expression datasets of primary DLBCLs in the context of miR-155 levels. Using supervised learning algorithms, we identified a robust gene signature driven by the differential expression of miR-155. These profiles contained several gene markers, including predicted targets, consistently downregulated in tumors expressing the high levels of miR-155. These data support the use of this strategy in the identification and validation of miRNA target genes.

Material and Methods

Cell lines and culture medium

The human DLBCL cell lines (SU-DHL4, SU-DHL5, SU-DHL6, SU-DHL7, SU-DHL8, SU-DHL10, OCI-Ly1, OCI-Ly4, OCI-Ly7, OCI-Ly8, OCI-Ly18, OCI-Ly19, DB, Farage, HT, Karpas-422, Pfeiffer, RC-K8, Toledo and WSU-NHL) were cultured at 37°C in 5% CO2 in RPMI-1640 medium (Mediatech) supplemented with 10% fetal bovine serum (FBS). OCI-Ly3 and OCI-Ly10 were maintained in Iscove's modified Dulbecco media with 20% FBS. All media contained penicillin (100U/mL), streptomycin (100μg/mL), L-glutamine (2mmol/L) and HEPES buffer (10 mmol/L).

RNA isolation and Northern blot analysis of mature microRNA

Total RNA was isolated from cultured cells using Trizol (Invitrogen) as described [10]. RNA quality was monitored by running aliquots of each sample in 1% agarose gel and by spectrophotometric analysis. Subsequently, forty micrograms of total RNA was run on 8M urea 15% polyacrylamide denaturing gels and transferred to nylon membranes (Genescreen plus, Perkin-Elmer) in a semi-dry apparatus. The resulting RNA filters were UV crosslinked

with 1000 μJ of energy (Stratagene UV Crosslinker) and hybridized overnight (ON) with the with antisense Starfire probe (IDT) for miR-155 (5′-CCCCTATCACGATTAGCATTAA-3′) and the control U6 small nucleolar RNA (snRNA) probe 5′-GCAGGGGCCATGCTAATCTTCTCTGTATCG-3′. After washing, membranes were placed in cassette with a blanked phosphoimager screen, exposed ON and developed on Typhoon 9410 phosphoimager (GE Healthcare). Densitometric quantification of the miRNA messages was performed with ImageQuant 5.2 (Molecular Dynamics).

Real-time quantitative RT-PCR (q-RT-PCR)

cDNA synthesis was performed using M-MLV Reverse Transcriptase (Promega) and 2.5μg of DNase-treated total RNA. For every sample, an identical reaction lacking the reverse-transcriptase enzyme was also included. The PCR amplifications were carried-out in triplicate using the SYBR green method in the iQ5 real-time PCR detection system (BioRad). In brief, we determined the expression of six gene transcripts in 22 DLBCL cell lines, including: two species of the pri-miR-155, the intron-free spliced mRNA (cytoplasmic) and the unspliced nuclear transcript (target of the Drosha/DGCR8 complex); two RNase III endonucleases, Drosha and Dicer, and two reference sequences, β-Actin and Cyclophilin A. The relative amount of the target genes (pri-miR-155, Drosha and Dicer) was calculated by subtracting the average C_T value for β-Actin or Cyclophilin from the average C_T value of each target gene (ΔCT). Subsequently, ΔΔCT values were calculated by subtracting the ΔC_T of the sample with the mean expression for each particular gene from the ΔC_T of each sample and expression defined as $2^{-\Delta\Delta CT}$. The range of expression levels was determined by calculating the standard deviation (s.d.) of the ΔCT, as described [10]. The primers sequences and PCR conditions are available upon request.

NF-KB activity assay

NF-κB activity was assessed in relevant DLBCL cell lines with an Elisa- (Enzyme-Linked ImmunoSorbent Assay) based colorimetric assay (Active Motif) that detects binding of cellular p50 (NF-κB1) to immobilized NF-κB target consensus oligonucleotide sequences. In brief, 2.5μg of whole-cell lysate was added to microwells containing immobilized NF-KB-specific target probes. Subsequently, cellular p50 bound to the immobilized NF-κB target sequences was detected using a p50-specific polyclonal antibody followed by an HRP-conjugated secondary antibody and colorimetric quantification. NF-κB binding activity in study samples was defined alongside that of standardized negative and positive controls provided by the manufacturer.

Data mining

To characterize pri-miR-155 transcript levels in primary DLBCLs we explored a publicly available microarray-based transcription dataset of 176 DLBCLs generated using Affymetrix U133A and U133B platforms[11]. Molecular classification into biologically-relevant molecular subgroups was available for all cases and included ABC, GC (Germinal Center) or Type 3 (COO, Cell-of-Origin classification) [12] DLBCLs as well as oxidative phosphorylation (OxPhos), B-cell receptor/proliferation (BCR) and host response (HR) tumors (CCC, Comprehensive Consensus Clustering classification)[11]. Data were normalized using the dChip software to achieve mean=0 and SD=1, as previously described [13]. The U133B Affymetrix chip contains two probe sets encompassing the *BIC* gene (pri-miR-155) locus: 229437_at and 233989_at. The 229437_at probe set maps to exon 3 of the *BIC* gene, where the precursor and mature miR-155 sequences are located. All 176 DLBCL samples had absolute (P) call for this probe set, which reflected the robustness of the signal. In contrast, most samples yielded an absent (A) call for probe 233989_at. The latter probe was thus excluded from the analysis. Normalized 229437_at values from the 176 tumors were used for further analysis.

Supervised Analysis of the DLBCL transcription dataset

To identify the genes that most accurately correlate with DLBCLs distinguished by high or low miR-155 expression, we used a supervised learning methods derived from the gene set enrichment analysis (GSEA) algorithm [14] and based on signal to noise metric and permutation tests. To enhance the specificity of this analysis, of the 176 DLBCLs present in our dataset only those at the 25th percentile of highest and lowest primary miR-155 expression (n=88) were used to generate this novel gene signature.

Statistical analysis

To measure the strength of the relationship between the expression of primary and mature miR-155 in the DLBCL cell lines we calculated Pearson correlation coefficients. The Kruskal-Wallis test was used to compare the medians of distributions of pri-miR-155 expression in tumors classified according to the COO and CCC molecular sub-groupings.

Results

Heterogeneous expression of mature miRNA-155 in the DLBCL cell lines

Using a specific and sensitive northern blot method, we found that the expression of mature miR-155 in DLBCL cell lines is heterogeneous (Figure 1a). Its relative expression, densitometrically quantified and normalized by the expression of the snRNA U6, allowed the classification of these cell lines into three groups: 4 cell lines expressed high levels, 9 low/intermediate levels and 9 had low/null expression of miR-155 (Figure 1a and Table 1). This heterogeneity suggests that in DLBCL miR-155 expression could represent a signature reminiscent of their cell of origin (ABC vs. GC-type DLBCL) and/or be associated with oncogenic events (e.g. NF-κB activation) present in subsets of DLBCLs [15]. However, the former appears less likely since of the four cell lines with the highest levels of miR-155 two are prototypic ABC-type lymphomas (OCI-Ly3 and OCI-Ly10) whereas the other two (RC-K8 and Farage) have been classified as GC-type. These data suggest that the expression of miR-155 in DLBCL is more complex than the dichotomization proposed in the ABC vs. GC sub-grouping. Therefore, to examine the role of the NF-κB pathway in the expression of miR-155, we measured its activity in eight DLBCL cell lines, including the four with the highest levels and 4 with low/null miR-155 expression. The miR-155 high cell lines showed a consistently higher NF-κB activity than the miR-155 low cell lines (p<.001) (Figure 2). These data suggest an association, if not a casual relationship, between NF-κB activity and miR-155 expression in DLBCL cell lines.

Expression of pri-miR-155 in DLBCL cell lines: Precise correlation between primary and mature miR-155

We were interested in defining whether measurements of pri-miR-155 (*BIC*) can be used as surrogate for the functional mature miR-155. To provide an additional level of dependability to our studies, we also defined the expression of the unspliced (nuclear) pri-miR-155 transcripts, as previously described[6]. In brief, gene expression levels defined by RT-PCR often reflect the abundance of cytosolic (spliced) transcripts. However, as the Drosha/DGCR8 complex is nuclear pri-miRNA transcripts targeted by this complex derive predominantly from unspliced RNA forms[1]. Consequently, spliced transcripts may not be the ideal pool of pri-miRNAs to be compared to mature miRNA. With that in mind, we developed an approach that specifically identifies spliced or unspliced pri-miR-155 isoforms. For the spliced qRT-PCR, primers were located in different exons of the *BIC* gene whereas for the unspliced assay one of the primers was intronic. In the latter, to confirm that the products amplified did not derive from DNA, all RNAs were treated with DNAse and the cDNA reaction lacking reverse-transcriptase (-RT) failed to yield any product (data not shown) when amplified alongside the

fully reverse-transcribed cDNA. Using this approach, we found (Figure 1b) that the amount of spliced cytosolic transcript closely reflects (r=.99) that of the unspliced pri-miR-155, which is preferentially subject to Drosha processing. Expectedly, given its abundance, the expression of the spliced form of pri-miR-155 was often higher than that of the unspliced transcript (Figure 1B). More importantly, we defined a marked correlation between the levels of pri-miR-155 and mature miR-155 transcripts in the DLBCL cell lines (r=.95 [DHL series], r=.94 [Ly series] and r=.97 [miscellaneous cell lines series]) (Figure 1). Finally, we found that Drosha and Dicer were expressed in all cell lines studied (data not shown) and that their abundance was largely independent of the primary or mature miR-155 levels (r=.32). Taken together, these data indicate that miRNA biogenesis is intact in DLBCL and that pri-miR-155 expression is a reliable surrogate for mature miR-155 levels.

miR-155 expression associates with specific DLBCL molecular sub-grouping

After confirming that in DLBCL the expression of pri- and mature miR-155 are highly correlated, we mined datasets of DLBCL generated with expression profiling platforms containing pri-miR-155 probes. One such dataset is an extensive molecular characterization of 176 well annotated nodal DLBCLs [11]. In that study, the pri-miR-155 probe set was ranked at the top 5-percentile of genes with the highest reproducibility within-duplicates and high variation across-patients (see Monti et al[11] for additional details). In brief, within-duplicate reproducibility shows that the expression measurement is reliable; high across-patients variation is evidence that the gene captures the variation in the sample population. The presence of pri-miR-155 among the 2118 genes at top 5-percentile indicates that this probe set effectively captures miR-155 expression.

To define whether the expression of miR-155 segregated with the molecular substructure of DLBCL, as defined by the COO or CCC classifications, we extracted and normalized the array data from 176 tumors classified as ABC (n=34), GC (n=85) Type 3 (n=57) – COO, or BCR (n=77), OxPhos (n=50) HR (n=49) – CCC. The expression of miR-155 was significantly higher (p<.0001, Kruskal-Wallis Test) in ABC than in GC or Type3 tumors (Figure 3, left panel). Conversely, there was no statistically significant difference (p=0.13, Kruskal-Wallis Test) in miR-155 expression when tumors were grouped by BCR, OxPhos, HR sub-types (Figure 3, right panel).

MiR-155 expression in a genome wide context: co-regulation with predicted targets

A link between miR-155 expression and that of putative target genes in DLBCL has not yet been reported. To start to address this issue, we used supervised learning algorithms to identify the genes that more clearly distinguished sub-groups of DLBCL dichotomized by the expression of pri-miR-155. Probe sets with a p < 0.0005 when corrected for multiple hypotheses testing (GSEA algorithm) determined the most stable gene signature (Figure 4). Because microRNAs function by attenuating the expression of target transcripts, we focus our attention on genes downregulated in DLBCLs expressing high levels of miR-155. This approach revealed a robust collection of 42 well-characterized gene markers whose expression inversely correlated with that of miR-155. Importantly, nine of the genes downregulated in miR-155 high tumors (fold of inhibition for the combined tumors in each class ranging from 10% to 54%, p<0.01) are predicted targets of this miRNA as defined by multiple models (TargetScan - http://www.targetscan.org, miRAnda -http://microrna.sanger.ac.uk/targets/v4/ and microCible - http://www.microarray.fr/microRNA/microcible/index.php) and at least three of them, KLRK1, AKAP10 and CSNK1G2, have been linked to a malignant phenotype [16–18]

Discussion

We found a precise correlation between the primary and mature miR-155 messages in DLBCL cell lines. These data suggest that miRNA biogenesis is intact in DLBCL and that pri-miR-155 expression is a reliable surrogate for mature miR-155 levels, allowing for a large scale characterization of miR-155 in primary DLBCLs previously studied gene expression profiling [11]. Our investigation of this dataset confirmed that miR-155 expression is significantly higher in ABC-type DLBCLs and importantly revealed a striking gene expression signature defined by the consistent downregulation of mRNA genes in DLBCL with high levels of miR-155.

We found a marked correlation between pri-miR-155 and mature miR-155 expression in DLBCL cell lines. Our findings differed from a recent report that indicated a lack of correlation between *BIC* transcript and mature miR-155 in DLBCL [6]. The reasons for this discrepancy are not immediately clear but could reflect the use of distinct technical approaches to measure mature miR-155, such as the PCR-based techniques used in the previous report, and the more specific northern blotting approach that we employed here. It is worth noting that for each measurement done in our study we selected the most robust technique available. Thus, we used Northern blot to measure the mature message and q-RT-PCR to define the pri-miR-155 levels, the state-of-the-art approach to define the correlation between two miRNA isoforms [9]. The correlation between the pri- and mature miR-155 and the steady expression of Drosha and Dicer strongly suggest that the miRNA biogenesis machinery is intact in these cell lines and that defective processing of pri-miR-155, as has been reported in Burkitt's cell lines [19], does not occur in DLBCL and does not account for the heterogeneous expression of mature miR-155 in this tumor.

In this study, we uncovered preliminary evidence suggesting that in DLBCL the expression of miR-155 could be driven by a constitutively active NF-kB pathway, as has been suggested for Burkitt's lymphoma [4,20,21]. In agreement with these findings, recent studies in murine mature B-cells [22] established that the Toll Like Receptors (TLRs)-mediated miR-155 induction is dependent on IKKgamma/NEMO, a member of the NF-κB pathway. Our findings suggest that it may be possible to extrapolate the data derived from these non-transformed cells to lymphoid malignancies such as DLBCL. Understanding these events is particularly relevant in light of the oncogenic role of miR-155 and the current efforts to develop clinical grade inhibitors to the NF-κB pathway.

In our series, miR-155 expression was significantly higher in ABC-tumors. These findings agree with previous reports that directly measured mature miR-155 in DLBCL [5–7] further supporting the reliability of pri-miR-155 as surrogate measure for mature miR-155 expression and strengthening the confidence on our measurements derived from expression profiling datasets. In addition, since ABC-tumors are known to associate with abnormal NF-κB signals these data agree with our findings in DLBCL cell lines.

Identification of mRNA genes directly (or indirectly) modified by miRNAs is an important step in understanding the function of these small regulatory molecules. One of the few large scale strategies available to address this problem is the use of gene expression arrays. However, this approach has relied mostly on the use of single cell lines modified to overexpress specific miRNAs [23] and has not been reported in association with datasets of primary tumors. Therefore, we reasoned that mining expression signatures of DLBCL could yield new and important preliminary insight on the activities of miR-155 in this tumor type. Using supervised learning algorithms, we defined a stable signature of genes that were downregulated in association with high expression of miR-155, including a significant fraction of predicted targets. These genes belong to various functional classes and comprise signal transduction molecules, structural proteins and transcription factors, without significant enrichment for any

particular group. Nonetheless, given the well established role of miR-155 in controlling immune system homeostasis, it is of interest that some of the targeted genes (e.g., KLRK1, TNFRSF7, LCK) are known to play a more direct role in immune function. These data raise the possibility that the oncogenic properties of miR-155 may at least partially derive from a faulty response by B-cells to micro-environmental cues within the germinal center and/or abnormal immune surveillance. While additional studies are necessary to define the mechanisms associated with miR-155 mediated lymphomagenesis our data should streamline these investigation by narrowing the number of candidate genes that may account for these effects.

References

1. Bartel DP. MicroRNAs: genomics, biogenesis, mechanism, and function. Cell 2004;116:281–97. [PubMed: 14744438]

2. Esquela-Kerscher A, Slack FJ. Oncomirs - microRNAs with a role in cancer. Nat Rev Cancer 2006;6:259–69. [PubMed: 16557279]

3. Metzler M, Wilda M, Busch K, Viehmann S, Borkhardt A. High expression of precursor microRNA-155/BIC RNA in children with Burkitt lymphoma. Genes Chromosomes Cancer 2004;39:167–9. [PubMed: 14695998]

4. van den Berg A, Kroesen BJ, Kooistra K, de Jong D, Briggs J, Blokzijl T, Jacobs S, Kluiver J, Diepstra A, Maggio E, Poppema S. High expression of B-cell receptor inducible gene BIC in all subtypes of Hodgkin lymphoma. Genes Chromosomes Cancer 2003;37:20–8. [PubMed: 12661002]

5. Kluiver J, Poppema S, de Jong D, Blokzijl T, Harms G, Jacobs S, Kroesen BJ, van den Berg A. BIC and miR-155 are highly expressed in Hodgkin, primary mediastinal and diffuse large B cell lymphomas. J Pathol 2005;207:243–9. [PubMed: 16041695]

6. Eis PS, Tam W, Sun L, Chadburn A, Li Z, Gomez MF, Lund E, Dahlberg JE. Accumulation of miR-155 and BIC RNA in human B cell lymphomas. Proc Natl Acad Sci U S A 2005;102:3627–32. [PubMed: 15738415]

7. Lawrie CH, Soneji S, Marafioti T, Cooper CD, Palazzo S, Paterson JC, Cattan H, Enver T, Mager R, Boultwood J, Wainscoat JS, Hatton CS. Microrna expression distinguishes between germinal center B cell-like and activated B cell-like subtypes of diffuse large B cell lymphoma. Int J Cancer 2007;121:1156–61. [PubMed: 17487835]

8. Costinean S, Zanesi N, Pekarsky Y, Tili E, Volinia S, Heerema N, Croce CM. Pre-B cell proliferation and lymphoblastic leukemia/high-grade lymphoma in E(mu)-miR155 transgenic mice. Proc Natl Acad Sci U S A 2006;103:7024–9. [PubMed: 16641092]

9. Thomson JM, Newman M, Parker JS, Morin-Kensicki EM, Wright T, Hammond SM. Extensive post-transcriptional regulation of microRNAs and its implications for cancer. Genes Dev 2006;20:2202–7. [PubMed: 16882971]

10. Smith PG, Wang F, Wilkinson KN, Savage KJ, Klein U, Neuberg DS, Bollag G, Shipp MA, Aguiar RC. The phosphodiesterase PDE4B limits cAMP-associated PI3K/AKT-dependent apoptosis in diffuse large B-cell lymphoma. Blood 2005;105:308–16. [PubMed: 15331441]

11. Monti S, Savage KJ, Kutok JL, Feuerhake F, Kurtin P, Mihm M, Wu B, Pasqualucci L, Neuberg D, Aguiar RC, Dal Cin P, Ladd C, Pinkus GS, Salles G, Harris NL, Dalla-Favera R, Habermann TM, Aster JC, Golub TR, Shipp MA. Molecular profiling of diffuse large B-cell lymphoma identifies robust subtypes including one characterized by host inflammatory response. Blood 2005;105:1851–61. [PubMed: 15550490]

12. Alizadeh AA, Eisen MB, Davis RE, Ma C, Lossos IS, Rosenwald A, Boldrick JC, Sabet H, Tran T, Yu X, Powell JI, Yang L, Marti GE, Moore T, Hudson J Jr, Lu L, Lewis DB, Tibshirani R, Sherlock G, Chan WC, Greiner TC, Weisenburger DD, Armitage JO, Warnke R, Levy R, Wilson W, Grever

MR, Byrd JC, Botstein D, Brown PO, Staudt LM. Distinct types of diffuse large B-cell lymphoma identified by gene expression profiling. Nature 2000;403:503–11. [PubMed: 10676951]

13. Dahia PL, Ross KN, Wright ME, Hayashida CY, Santagata S, Barontini M, Kung AL, Sanso G, Powers JF, Tischler AS, Hodin R, Heitritter S, Moore F, Dluhy R, Sosa JA, Ocal IT, Benn DE, Marsh DJ, Robinson BG, Schneider K, Garber J, Arum SM, Korbonits M, Grossman A, Pigny P, Toledo SP, Nose V, Li C, Stiles CD. A HIF1alpha regulatory loop links hypoxia and mitochondrial signals in pheochromocytomas. PLoS Genet 2005;1:72–80. [PubMed: 16103922]

14. Subramanian A, Tamayo P, Mootha VK, Mukherjee S, Ebert BL, Gillette MA, Paulovich A, Pomeroy SL, Golub TR, Lander ES, Mesirov JP. Gene set enrichment analysis: a knowledge-based approach for interpreting genomewide expression profiles. Proc Natl Acad Sci U S A 2005;102:15545–50. [PubMed: 16199517]

15. Davis RE, Staudt LM. Molecular diagnosis of lymphoid malignancies by gene expression profiling. Curr Opin Hematol 2002;9:333–8. [PubMed: 12042708]

16. Kaiser BK, Yim D, Chow IT, Gonzalez S, Dai Z, Mann HH, Strong RK, Groh V, Spies T. Disulphide-isomerase-enabled shedding of tumour-associated NKG2D ligands. Nature 2007;447:482–6. [PubMed: 17495932]

17. Denning KM, Smyth PC, Cahill SF, Finn SP, Conlon E, Li J, Flavin RJ, Aherne ST, Guenther SM, Ferlinz A, O'Leary JJ, Sheils OM. A molecular expression signature distinguishing follicular lesions in thyroid carcinoma using preamplification RT-PCR in archival samples. Mod Pathol. 2007

18. Wirtenberger M, Schmutzhard J, Hemminki K, Meindl A, Sutter C, Schmutzler RK, Wappenschmidt B, Kiechle M, Arnold N, Weber BH, Niederacher D, Bartram CR, Burwinkel B. The functional genetic variant Ile646Val located in the kinase binding domain of the A-kinase anchoring protein 10 is associated with familial breast cancer. Carcinogenesis 2007;28:423–6. [PubMed: 16956908]

19. Kluiver J, van den Berg A, de Jong D, Blokzijl T, Harms G, Bouwman E, Jacobs S, Poppema S, Kroesen BJ. Regulation of pri-microRNA BIC transcription and processing in Burkitt lymphoma. Oncogene. 2006

20. Kluiver J, van den Berg A, de Jong D, Blokzijl T, Harms G, Bouwman E, Jacobs S, Poppema S, Kroesen BJ. Regulation of pri-microRNA BIC transcription and processing in Burkitt lymphoma. Oncogene 2007;26:3769–76. [PubMed: 17173072]

21. O'Connell RM, Taganov KD, Boldin MP, Cheng G, Baltimore D. MicroRNA-155 is induced during the macrophage inflammatory response. Proc Natl Acad Sci U S A 2007;104:1604–9. [PubMed: 17242365]

22. Thai TH, Calado DP, Casola S, Ansel KM, Xiao C, Xue Y, Murphy A, Frendewey D, Valenzuela D, Kutok JL, Schmidt-Supprian M, Rajewsky N, Yancopoulos G, Rao A, Rajewsky K. Regulation of the germinal center response by microRNA-155. Science 2007;316:604–8. [PubMed: 17463289]

23. Lim LP, Lau NC, Garrett-Engele P, Grimson A, Schelter JM, Castle J, Bartel DP, Linsley PS, Johnson JM. Microarray analysis shows that some microRNAs downregulate large numbers of target mRNAs. Nature 2005;433:769–73. [PubMed: 15685193]

24. Lenz G, Nagel I, Siebert R, Roschke AV, Sanger W, Wright GW, Dave SS, Tan B, Zhao H, Rosenwald A, Muller-Hermelink HK, Gascoyne RD, Campo E, Jaffe ES, Smeland EB, Fisher RI, Kuehl WM, Chan WC, Staudt LM. Aberrant immunoglobulin class switch recombination and switch translocations in activated B cell-like diffuse large B cell lymphoma. J Exp Med 2007;204:633–43. [PubMed: 17353367]

25. Pasqualucci L, Guglielmino R, Houldsworth J, Mohr J, Aoufouchi S, Polakiewicz R, Chaganti RS, Dalla-Favera R. Expression of the AID protein in normal and neoplastic B cells. Blood 2004;104:3318–25. [PubMed: 15304391]
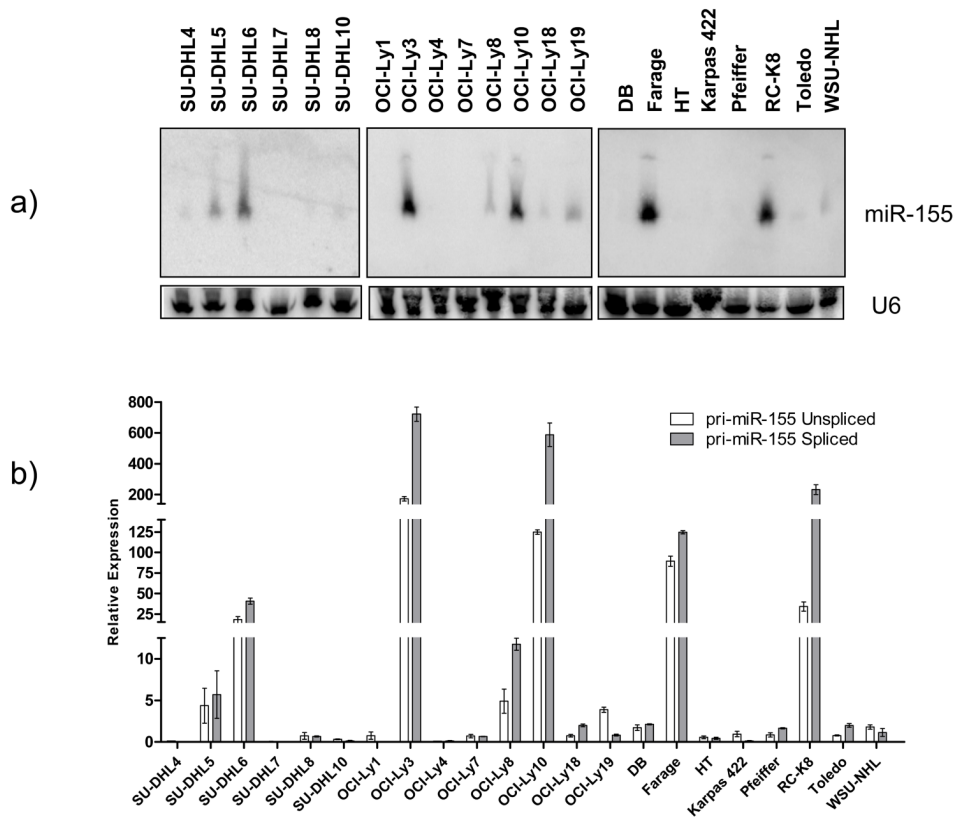
Figure 1. Expression of mature and primary miR-155 in DLBCL cell lines
Mature and primary (unspliced and spliced) miR-155 expression was defined by northern blot
(a) and q-RT-PCR (b), respectively. Densitometric quantification of the mature miRNA
messages was performed with ImageQuant 5.2 (Molecular Dynamics) and normalized by the
expression of the snRNA U6. The primary miR-155 expression was normalized by the
expression of cyclophilin A. Pearson correlation coefficients between primary and mature
miR-155 were .95 (DHL series), .94 (Ly series) and .97 (miscellaneous series).
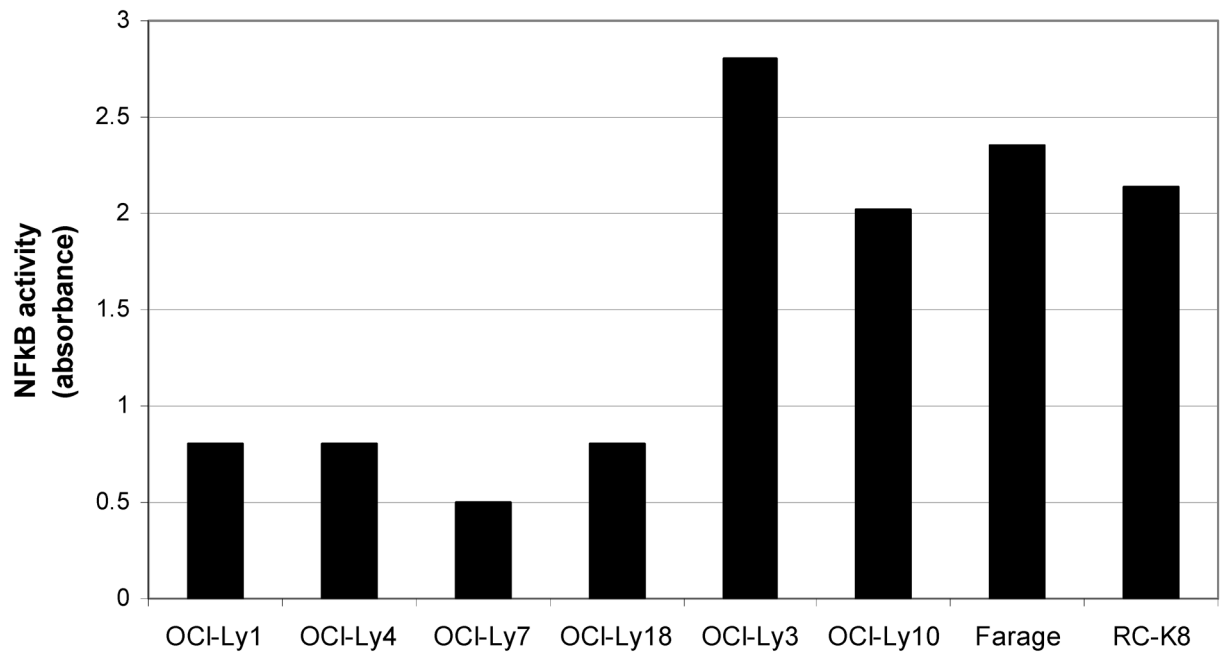
Figure 2. NF-κB activity of DLBCL cell lines expressing distinct levels of miR-155
The NFκB activity was significantly lower in cell lines OCI-Ly1, OCI-Ly4, OCI-Ly7 and OCI-Ly18 with low/null miR-155 expression than in the high miR-155 lines, OCI-Ly3, OCI-LY10, Farage and RC-K8 (p<.001)
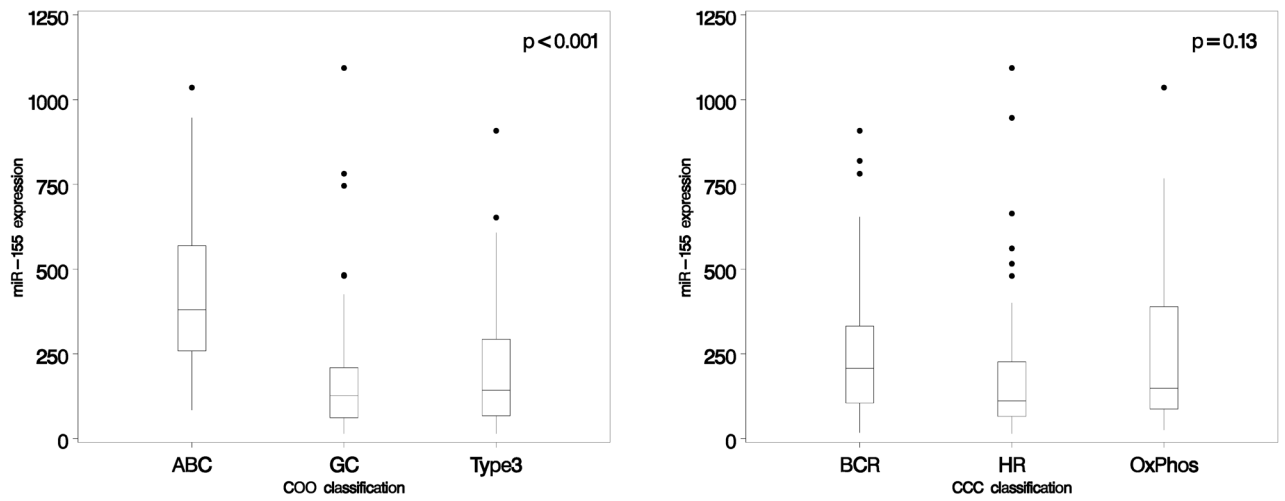
Figure 3. Distribution of pri-miR-155 expression by COO (left) and CCC classification (right)
In the box plots, the outliers samples (those whose expression extends beyond 1.5 times the inter-quartile range) are noted as dots. P-values (Kruskal-Wallis test) are shown in the right upper corner on the panels.
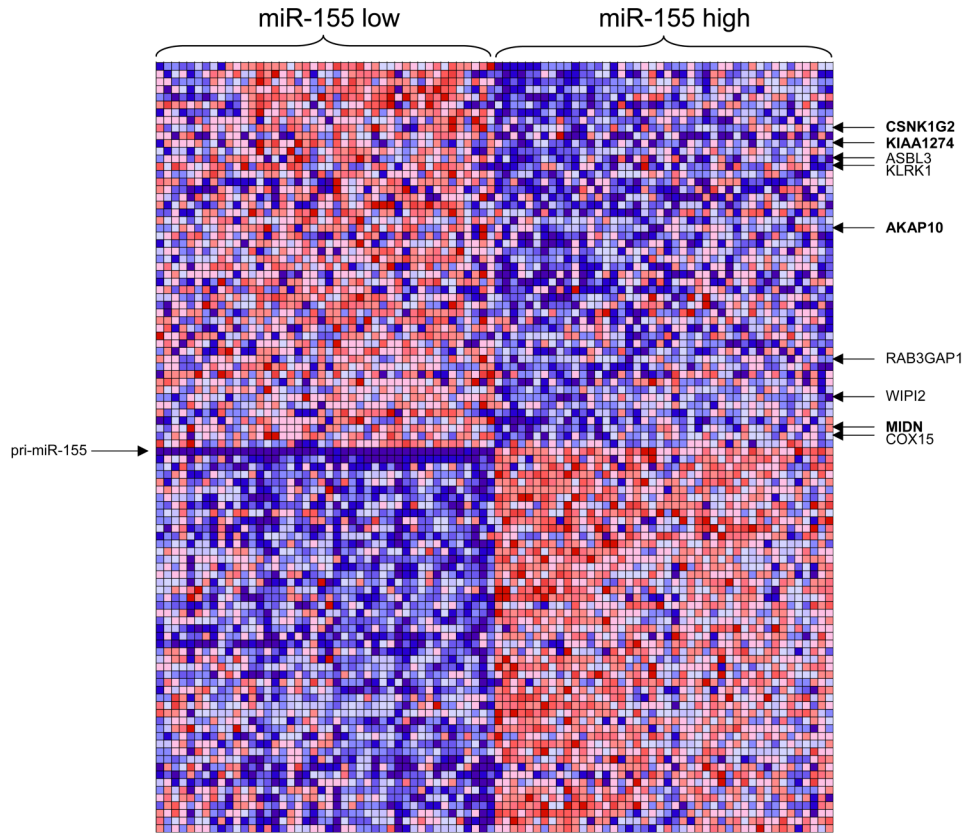
Figure 4. Gene signature of DLBCL dichotomized by the expression of miR-155
The 100 probe sets that more strongly correlate with miR-155 expression in 88 DLBCLs are shown. Gene ranks are based on signal-to-noise metrics and red or blue indicate high or low expression, respectively. Each column is a tumor and each row a gene. The genes consistently downregulated in DLBCL expressing high miR-155 levels are shown of the upper right quadrant. The predicted miR-155 targets, distributed throughout this ranked group, are indicated (in bold are those predicted by multiple models). Expectedly, expression of MiR-155, indicated on the left, drives the distinction between these two DLBCL groups.

Table 1

Mature miR155 expression in DLBCL cell lines

Normalized densitometric quantification of miR-155 message allowed stratification of these cell lines in three groups expressing low (densitometric units <6), low/intermediate (6–40) or high levels of miR-155(>40). Classification of these cell lines according to the COO molecular substructure has been reported earlier [12,24,25].

Cell line	DLBCL subtype	Mature miR-155 expression	Densitometry[*]
SU-DHL4	GCB	Low	1.58
SU-DHL5	ND	Intermediate	7.54
SU-DHL6	GCB	Intermediate	12.86
SU-DHL7	ND	Low	2.00
SU-DHL8	ND	Intermediate	1.94
SU-DHL10	GCB	Low	2.05
OCI-Ly1	GCB	Low	3.56
OCI-Ly3	ABC	High	85.73
OCI-Ly4	GCB	Low	5.18
OCI-Ly7	GCB	Low	2.89
OCI-Ly8	GCB	Intermediate	7.62
OCI-Ly10	ABC	High	55.25
OCI-Ly18	GCB	Intermediate	6.98
OCI-Ly19	GCB	Intermediate	10.42
DB	GCB	Low	3.46
Farage	GCB	High	47.16
HT	GCB	Low	4.09
Karpas 422	ND	Low	4.20
Pfeiffer	ND	Intermediate	7.01
RC-K8	GCB	High	94.15
Toledo	GCB	Intermediate	6.94
WSU-NHL	ND	Intermediate	10.75

ND- not determined.

[*] arbitrary units